High ambient contrast ratio OLED and QLED without a circular polarizer

Guanjun Tan[1]**, Ruidong Zhu**[1]**, Yi-Shou Tsai**[2]**, Kuo-Chang Lee**[2]**, Zhenyue Luo**[1]**, Yuh-Zheng Lee**[2] **and Shin-Tson Wu**[1]

[1] College of Optics and Photonics, University of Central Florida, Orlando, FL 32816, USA
[2] Display Technology Center, Industrial Technology Research Institute, Hsinchu 31040, Taiwan

E-mail: swu@ucf.edu

CrossMark

Abstract

A high ambient contrast ratio display device using a transparent organic light emitting diode (OLED) or transparent quantum-dot light-emitting diode (QLED) with embedded multilayered structure and absorber is proposed and its performance is simulated. With the help of multilayered structure, the device structure allows almost all ambient light to get through the display device and be absorbed by the absorber. Because the reflected ambient light is greatly reduced, the ambient contrast ratio of the display system is improved significantly. Meanwhile, the multilayered structure helps to lower the effective refractive index, which in turn improves the out-coupling efficiency of the display system. Potential applications for sunlight readable flexible and rollable displays are emphasized.

Keywords: organic light emitting diode, quantum dots, sunlight readability

(Some figures may appear in colour only in the online journal)

1. Introduction

Thin-film-transistor liquid crystal display (LCD) and organic light emitting diode (OLED) are now two dominating display technologies. LCDs have been widely used in smartphones, tablets, televisions and other display devices, with advantages of low cost, long lifetime, relatively high ambient contrast ratio (ACR), and wide color gamut with a quantum-dot (QD) backlight [1–3]. While OLEDs exhibit advantages in true black state, vivid colors, good flexibility, and fast response time [4–6]. In spite of all these advantages, sunlight readability of OLEDs is still quite limited because of the strong reflection from the inner metallic electrodes. In order to improve ACR, circular polarizer (CP) has been commonly used in OLED display systems to suppress ambient light reflection [7]. Although CP helps to mitigate reflection to 4–6%, it causes some drawbacks [8], such as more than 50% absorption loss of the OLED output efficiency, decreased flexibility, and increased cost. Thus, a thin CP with low absorption loss yet high CR is favorable for flexible OLED displays. Recently, an ultra-thin linear polarizer [9] has been developed, which provides a potential solution for high ACR flexible OLED displays. Several other approaches have also been proposed to reduce

the reflectance and increase the ACR of an OLED display [10], for instance, black cathode [11–15], absorbing transport layer [16, 17], destructive interference structures [18–20] and black matrix [21]. However, most of these methods have trade-offs in providing a similar luminous reflectance to CP while keeping a high out-coupling efficiency. Moreover, in some of these approaches, additional layers are needed in the electrical active region, which would undesirably affect the OLED's electrical properties and lifetime. Recently, quantum dot light-emitting diode (QLED) is emerging, which offers another choice for next generation flexible displays [22]. A QLED has similar layered structure to OLED, thus, it would also suffer from the same sunlight readability issue.

In this paper, we propose a new high ACR display device, which consists of a transparent OLED (or QLED) with embedded multilayered structure and an absorber. The transparent OLED or QLED [23] is comprised of two transparent electrodes. The multilayered structure is embedded in the transparent OLED or QLED, and then an absorber is arranged to the opposite side of the multilayer. The thicknesses and materials of the multilayer can be well optimized to reach the destructive interference for the whole structure. And then, with the help of the multilayered structure, the whole
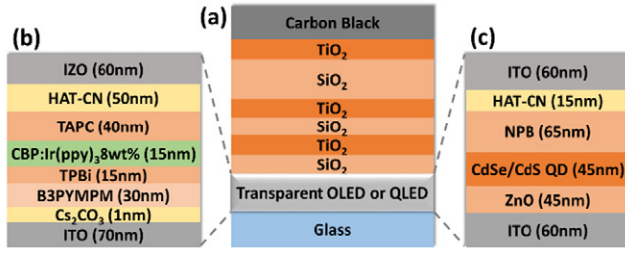
Figure 1. (a) Proposed high ACR device structure, (b) transparent OLED stack, and (c) transparent QLED stack.

Figure 2. Transparent OLED: (a) PL spectrum of 8 wt% Ir(ppy)$_3$ doped CBP taken from [19], and (b) our simulation results on the amount of power coupled to different optical channels.

Figure 3. Transparent QLED: (a) PL spectrum of CdSe/CdS QDs taken from [21], and (b) our simulation results on the amount of power coupled to different optical channels.

device works as an anti-reflection (AR) structure and allows all ambient light to get through the display and be absorbed by the absorber, instead of being reflected by the metallic electrode. As a result, the reflected ambient light is greatly reduced, and the ACR of the display system is improved significantly. Meanwhile, the optimized multilayered structure also helps lower the effective refractive index, which in turn distributes more energy to the substrate mode and direct emission. So the multilayered structure also improves the out-coupling efficiency of the display system. This new high contrast display device shows several advantages in comparison with prior arts: (1) quite low luminous reflectance (~1%), (2) high efficiency for direct emission and substrate modes when combined with a high index substrate, (3) no effect on the electrical properties of OLED or QLED because the structure is integrated outside the electrical active region, (4) low color shift, and (5) thin and flexible because no CP is used.

2. Device structure

2.1. High ambient contrast OLED and QLED

The cross-sectional view of proposed high ACR display device is shown in figure 1(a). The multilayered structure, is deposited on the transparent OLED or QLED, and an absorber (e.g. carbon black) is laminated unto the multilayered structure. The material used in the multilayer can be two or more dielectric media with different refractive indices, for example, SiO$_2$ and TiO$_2$. And the thickness of each layer needs to be optimized in order to minimize reflectance and enhance optical efficiency.

2.2. Transparent OLED and QLED

Figures 1(b) and (c) show the structures of transparent OLED and QLED, respectively. The transparent OLED in figure 1(b) has been demonstrated experimentally [23]. It has an inverted structure with two transparent electrodes: ITO and IZO. The green light emitting layer material is 8 wt% Ir(ppy)$_3$ [fac-tris(2-phenylpyridine) iridium] doped CBP [4,4′-N,N′-dicarbazole-biphenyl], whose PL spectrum is depicted in figure 2(a). Figure 1(c) shows the device structure of the proposed transparent QLED. Such structure is similar to that proposed in [24, 25]; the only difference is that the top aluminum electrode in the original structure is replaced by ITO to make it transparent to visible light. A cadmium selenide-cadmium
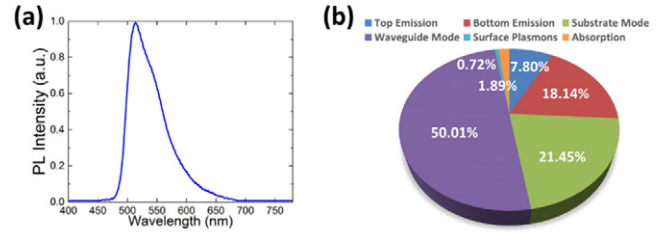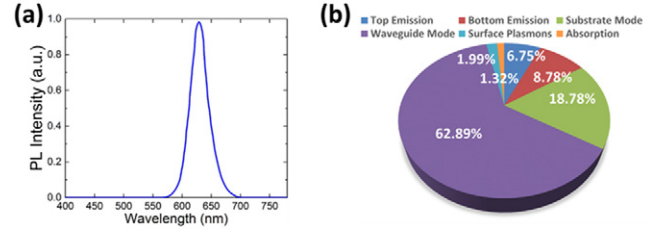
sulfide (core-shell) quantum dot layer is used as the emitting layer (EML). The PL spectrum of the QD emitting layer is shown in figure 3(a).

Here we use dipole model [26] to evaluate the out-coupling efficiency and angular dependence of the OLED and QLED structures. The dipole model was first developed to simulate the light emission spectra of OLED, in which the EQE is defined as [27]:

$$\mathrm{EQE} = \eta \cdot \mathrm{IQE} = \eta \cdot \gamma \cdot \eta_{\mathrm{S/T}} \cdot q_{\mathrm{eff}}, \qquad (1)$$

where η is the outcoupling efficiency and IQE is the internal quantum efficiency, which is the product of effective quantum yield q_{eff}, charge carrier balance γ, and singlet/triplet capture ratio $\eta_{\mathrm{S/T}}$ [28]. In this paper, our main purpose is to analyze the optical out-coupling efficiency of OLEDs and QLEDs. Without losing generality, let us assume internal quantum efficiency is unitary.

The quantitative power dissipation of OLEDs and QLEDs can be simulated by the dipole model [26, 27]. Both transverse magnetic (TM) and transverse electric (TE) waves are taken into consideration in the dipole model. The power dissipation density K can be calculated for randomly oriented dipoles as:

$$K = \frac{1}{3} K_{\mathrm{TM}v} + \frac{2}{3} (K_{\mathrm{TM}h} + K_{\mathrm{TE}h}), \qquad (2)$$

where the subscripts v and h represent the dipoles parallel to the z axis and the x-y plane, respectively. More detailed description of each term in equation (2) can be found in [25]. The optical channels are separated by their in-plane wave vector k_x: (1) direct emission (or air mode), depicting the light directly emitting into air when $0 \leqslant k_x \leqslant k_0 \cdot n_{\mathrm{air}}$ ($k_0 = 2\pi/\lambda$ is the vacuum wave vector); (2) substrate mode, showing light trapped in substrate due to total internal reflection (TIR) when $k_0 \cdot n_{\mathrm{air}} < k_x \leqslant k_0 \cdot n_{\mathrm{sub}}$; (3) waveguide mode, showing light guided inside the organic/inorganic hybrid layers, when

J. Phys. D: Appl. Phys. **49** (2016) 315101

G Tan *et al*
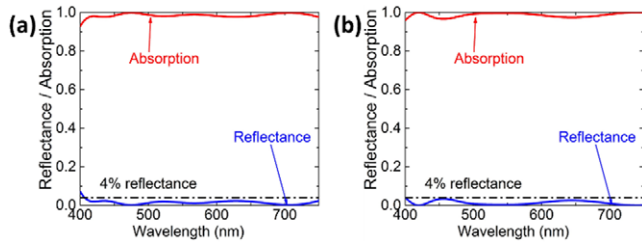
Figure 4. Simulated reflectance and absorption of the proposed high ACR device in the visible spectral region: (a) OLED and (b) QLED.

$k_0 \cdot n_{sub} < k_x \leqslant k_0 \cdot n_{eff}$, where n_{eff} is the real part of the equivalent refractive index of the organic/inorganic hybrid layers and ITO layer (the metallic layer and the glass substrate layer are not included). The expression for n_{eff} is:

$$\varepsilon_{eff} = \sum_i d_i / \sum_i (d_i / \varepsilon_i),$$
$$n_{eff} = \mathrm{Re}(\sqrt{\varepsilon_{eff}}). \qquad (3)$$

In equation (3), d_i is the layer thickness, ε_i is the corresponding complex dielectric constant, and ε_{eff} is the equivalent dielectric constant. (4) Surface plasmons mode, corresponding to the evanescent wave at the organic/metal interface, when $k_0 \cdot n_{eff} < k_x$. The simulation results of energy mode distribution of two transparent structures in figure 1 are shown in figures 2(b) and 3(b).

The EQE of the simulated OLED structure is 26%, with 7.80% for top emission and 18.14% for bottom emission. The simulated results match well with those reported in [23]. For the proposed transparent QLED, the EQE is about 16%. Most of the light power is trapped in substrate mode and waveguide mode. This amount of light can be extracted by either internal or external extraction strategies. For these two structures, the fraction of power dissipating in surface plasmons mode and absorption is quite small, due to the transparent electrodes instead of metal electrodes.

3. Low reflectance

Firstly, we optimize the multilayers of the proposed high ACR OLED and QLED devices with glass BK7 ($n \sim 1.5$) as substrate, six SiO_2/TiO_2 layers as multilayer and carbon black as absorber. We maintain the thicknesses of OLED/QLED to avoid distortion of electrical properties and then optimize the thicknesses of the six layers to get low reflectance while keeping high EQE. The optimized high ACR OLED structure is BK7/transparent OLED/SiO_2 (5 nm)/TiO_2 (48 nm)/SiO_2 (18 nm)/TiO_2 (17 nm)/SiO_2 (152 nm)/TiO_2 (10 nm)/Carbon Black. Similarly, after optimization the high ACR QLED structure is BK7/transparent QLED/SiO_2 (38 nm)/TiO_2 (10 nm)/SiO_2 (63 nm)/TiO_2 (3 nm)/SiO_2 (145 nm)/TiO_2 (15 nm)/Carbon Black. Both structures show a low reflectance (<4%) over the entire visible spectrum (figure 4). In our reflectance calculation, we neglect the surface reflection between glass substrate and air interface, by assuming it has a perfect anti-reflection (AR) coating.
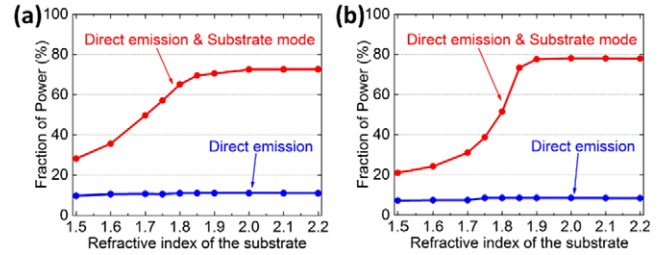
Figure 5. Optical efficiency of high ACR devices with different refractive index (n_s) of substrate: (a) OLED and (b) QLED.

We also calculate the luminous reflectance defined as:

$$R_L = \frac{\int_{\lambda_1}^{\lambda_2} V(\lambda) R(\lambda) S(\lambda) \mathrm{d}\lambda}{\int_{\lambda_1}^{\lambda_2} V(\lambda) S(\lambda) \mathrm{d}\lambda}, \qquad (4)$$

where $V(\lambda)$ is the spectral eye sensitivity, $R(\lambda)$ is the reflectance of the device, and $S(\lambda)$ is the spectrum of ambient light. The calculated luminous reflectance, 1.52% for high contrast OLED and 0.85% for high contrast QLED, are both low enough to displace circular polarizer. But at the same time, the optical efficiency should also be considered. For the proposed OLED, the direct emission is 9.70% and substrate mode is 18.42%, while for QLED the direct emission is 7.29% and substrate mode is 13.71%. Considering more than 50% loss of circular polarizer, our high ACR OLED and QLED can achieve same efficiency as a conventional OLED and QLED but with greater flexibility.

4. High efficiency

Please note that in the optimized multilayer, the total thickness of low refractive index material SiO_2 is much larger than that of high refractive index material TiO_2. So, the effective refractive index of entire structure would be reduced by adopting the multilayer. The lower effective refractive index helps distribute more energy to the substrate mode and direct emission, if we use a high refractive index substrate [29].

Next, we explore how a high refractive index (n_s) substrate enhances the outcoupling of both direct emission and substrate mode [30, 31]. With outcoupling structures such as micro-extractors, most of the substrate mode can be extracted. During simulation we increase substrate refractive index and optimize the multilayers for each n_s and then calculate the reflectance and efficiency. Figure 5 shows the fraction of power for both direct emission and substrate mode under different n_s, while keeping the luminous reflectance as low as ~1%. As figure 5 shows, efficiency increases and then gradually saturates as n_s increases. The combined efficiency of direct emission and substrate mode can exceed 70%, which conventional CP-based OLED and QLED cannot reach because more than 50% of the emitted light is absorbed by the employed circular polarizer. From figure 5, the efficiency starts to saturate when $n_s \geqslant 1.85$. A higher n_s substrate is more costly. Thus, we choose $n_s = 1.85$ to investigate the angular dependence of the proposed structure. With $n_s = 1.85$, the luminous reflectance remains quite low; 1.13% for OLED and 0.77% for QLED.

J. Phys. D: Appl. Phys. **49** (2016) 315101

G Tan *et al*
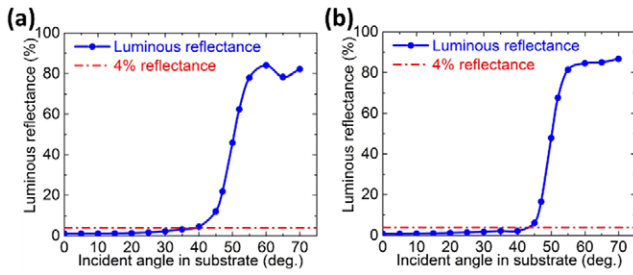
Figure 6. Luminous reflectance for ambient light with different incident angle in the substrate: (a) high contrast OLED and (b) high contrast QLED.

5. Angular dependence

5.1. Large angle incident light

As analyzed above, the reflectance keeps quite low for normally incident ambient light. But large angle should be analyzed as well. Figure 6 shows the luminous reflectance for light with different incident angles (in the substrate). We know that the angle inside the substrate is correlated to the angle in the air by Snell's law. For a flat surface, by simple calculation, the ambient light incident from the air will be confined within 0–32.7° in the substrate. From figure 6, we can see that in this angular range, the luminous reflectance still keeps less than 4%. So the proposed structures can maintain low reflectance for large angle incident light from the air.

5.2. Color shift

For some thin-film devices, such as OLEDs and QLEDs, the color performance of a micro-cavity structure could vary strongly depending on the viewing angle. The thicknesses of the transparent OLED and QLED are both ~300 nm and the total thickness of the high ACR OLED and QLED is about 550 nm. Here, we evaluate the color shift of our devices and results are plotted in figure 7. From figure 7, the color shift $\Delta\mu'\nu'$ is less than 0.002, which is much smaller than that of commercial OLED products. An important reason that our proposed structures show negligible angular dependency is due to its weak cavity effect, in comparison with conventional OLEDs and QLEDs.

6. Discussion

6.1. Function of multilayered structure

From above discussion, the multilayered structure plays an important role to lower the device reflectance and enhance the device efficiency. But the function of multilayered structure still needs to be investigated clearly and quantitatively. Here we compare two OLED structures with $n_s = 1.85$. The first one is our proposed transparent OLED with multilayered structure and carbon black (figure 1(a)) and the second one is just a transparent OLED with an absorber directly deposited on the top IZO electrode, without the multilayered structure. The simulated reflectance and efficiency of these two
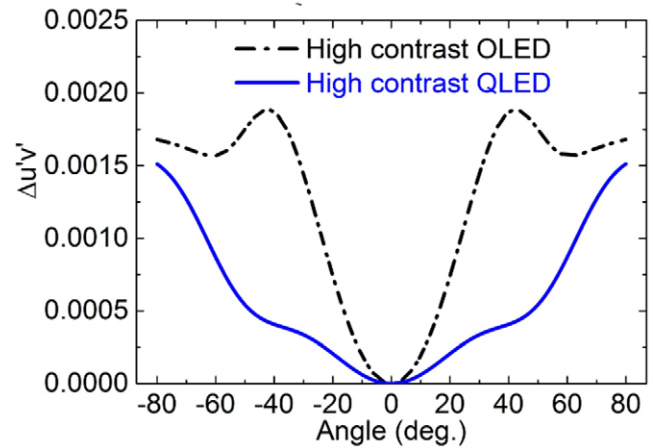
Figure 7. Calculated color shift of the proposed high ACR OLED and QLED.

structures are plotted in figure 8. We find that the adoption of multilayered structure can further suppress the reflectance from 5.43% to 1.13% and improve the efficiency because the absorption is reduced and the energy in substrate mode is also improved greatly.

An important reason why the multilayered structure can enhance the efficiency is that it helps lower the effective refractive index. The effective refractive index of the organic layers before adopting multilayer is 1.82, but with the help of multilayer the effective refractive index is reduced to 1.67 at $\lambda = 520$ nm. From waveguide optics, such a decreased effective refractive index increases the energy confined in the high index substrate. This is the reason why adopting a high index substrate can help extract more energy into substrate [30, 31]. After comparing our simulation results, we can confidently claim that multilayered structure serves two important purposes: (1) it leads to a much lower reflectance, and (2) it improves light efficiency.

6.2. Trade-off between reflectance and efficiency

When we optimize the multilayered structure, there appears an obvious trade-off between low reflectance and high efficiency. The reason is easy to understand. In order to lower reflectance, we need to optimize the multilayer to allow more ambient light to get through the device and be absorbed by the absorber. However, this would also lead to more absorption of OLED and QLED emission. Consequently, the trade-off between reflectance and efficiency exists. To get clear understanding of the trade-off, quantitative analysis is necessary. For such a multi-objective problem, any further improvement of the solution in terms of one objective is likely to be compromised by the degradation of another objective. Such solutions constitute a so-called *Pareto front* [32]. Figure 9 shows the *Pareto fronts* of proposed OLED and QLED with glass BK7 as substrate. Each point in the blue line in figures 9(a) and (b) corresponds to an optimized structure with best efficiency we can achieve at certain reflectance. From figure 9, we can easily see that when the luminous reflectance decreases, the direct emission would also decrease accordingly. When we keep

J. Phys. D: Appl. Phys. **49** (2016) 315101

G Tan *et al*
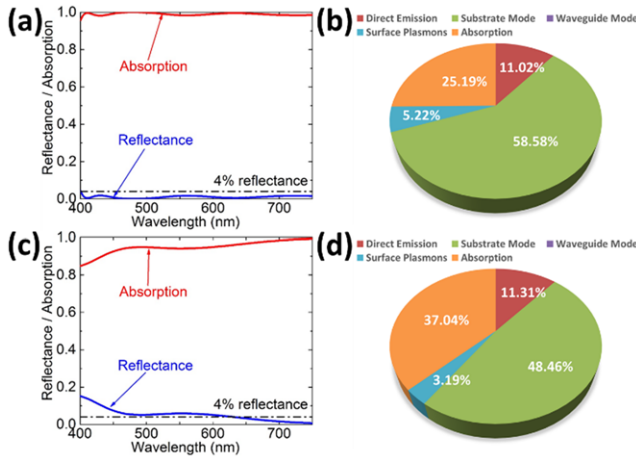
Figure 8. The first structure: (a) calculated reflectance with luminous reflectance 1.13% and (b) simulated result of the amount of power coupled to different optical channels. The second structure: (c) calculated reflectance with luminous reflectance 5.43% and (d) simulated result of the amount of power coupled to different optical channels.
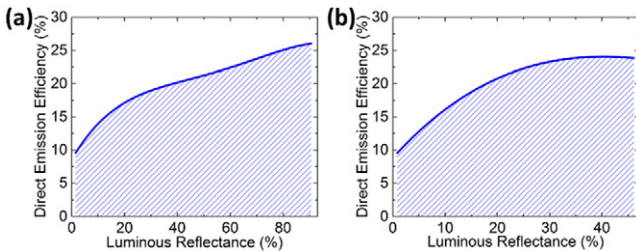
Figure 9. Trade-off between reflectance and efficiency: (a) relationship between luminous reflectance and direct emission efficiency of the proposed high contrast OLED structure with BK7 glass substrate, and (b) for QLED with BK7 glass substrate.

luminous reflectance less than 4%, the highest direct emission efficiency for OLED is 11.07% and the highest efficiency for QLED is 12.08%. These two curves help us to get optimal structure under different requirements.

6.3. Effects of microstructure

As mentioned above, after employing the high index substrate, we still need microstructure to extract the enhanced substrate mode energy. In this section, we investigate the effects of microstructure on out-coupling efficiency and reflectance in detail. For consistency, we still use OLED as an example to analyze the effects of microstructure. The simulation of OLEDs with microstructure as external extractor can be taken in two steps: (1) emission into the substrate and (2) light propagation in the substrate [33]. The emission in the substrate can be calculated with dipole model, as clearly stated above. The propagation of light in the substrate needs to be simulated by ray tracing model because its thickness is usually in the order of millimeter and optical interference effects play no role. We use commercial ray tracing programs Light Tools to accomplish the light propagation simulation.

We tried two simple microstructures, microlens and micro pyramid array, as examples to evaluate the microstructure
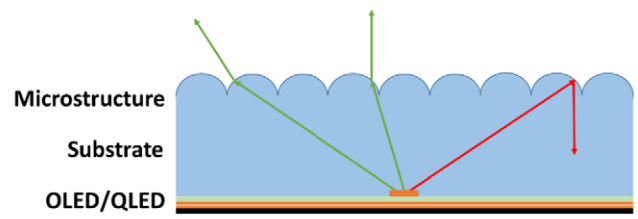
Figure 10. Geometrical representation of a high contrast OLED with microstructure as out-coupling extractor.

Table 1. Efficiency enhancement for OLED with microstructures.

Device structure	EQE by dipole model (%)	Enhancement ratio by light tools	Simulated EQE (%)
Reference	11.02	—	11.02
Micro lens array	—	2.16	23.78
Micro pyramid array	—	1.78	19.63
Hemisphere lens	69.60[a]	6.31	69.58

[a] This value is the summation of the power dissipations to air mode and substrate mode under the assumption that both modes can be extracted by the hemi-spherical lens.

effects. Figure 10 depicts the geometrical representation of the whole structure.

We simulated the efficiency enhancement of OLED with microlens and micro pyramid array and results are listed in table 1. The microlens array is implemented as spherical caps whose base radius is 50 μm and height is 35 μm. The micro pyramid array consists of four sided pyramids with a square base measuring 100 × 100 μm^2 and height 40 μm. For both structures, the distance between two neighboring elements is 100 μm.

From the simulated data, both microlens and micro pyramid arrays can enhance the out-coupling efficiency as expected. And keep in mind that the efficiency is already 2× higher than that using a circular polarizer. Meanwhile, the use of microstructures would also change the reflectance of the display. Figure 11 depicts the simulated luminous reflectance of the whole structure.

For comparison, we used the structure with planer surface and perfect AR coating as reference. Firstly, we calculated the reflectance of CP-based OLED at different viewing angle. The circular polarizer we used consists of a linear polarizer, a half-wave plate and a quarter-wave plate [34]. From figure 11, the structures with both microstructures can still maintain a fairly low reflectance (<4%) if the incident light is within ~40°. As the angle increases, the total reflectance increases. The reason is that the adoption of microstructure would change the angular distribution of ambient light in substrate. Our multilayered structure shows a higher reflectance for large incident angle, as figure 6 depicts. Thus, the total reflection of the proposed structure increases at large angles. To suppress the reflectance at large angles, we could optimize the microstructure shape and dimension, however the trade-off between low reflectance and high efficiency still exists. Another approach is to weaken
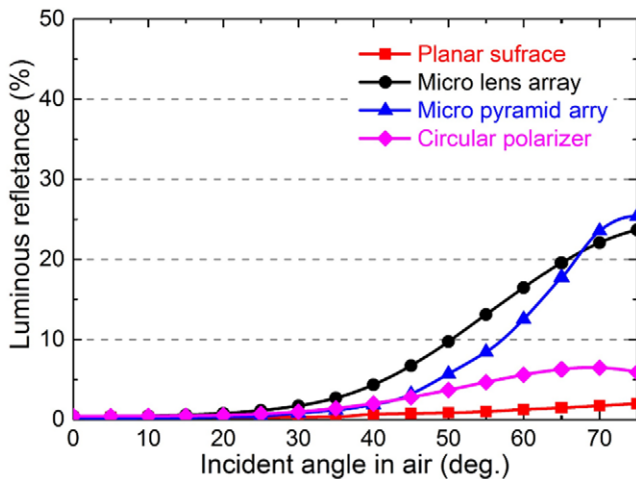
Figure 11. Luminous reflectance of high contrast OLED with microstructures for ambient light with different incident angle in air.

the angular dependence of the multilayered structure. This can be realized by using more TiO_2/SiO_2 layers in the multilayered structure.

7. Conclusion

High ambient contrast ratio display devices using transparent OLED or quantum-dot LED with an embedded multilayered structure and a black absorber are proposed. The performance of the proposed structure is analyzed in detail. Both devices show quite low luminous reflectance (~1%), high efficiency, and negligible color shift. Our devices do not need a circular polarizer, and therefore it opens a new door for next generation flexible and rollable display applications.

Acknowledgments

References

[1] Bourzac K 2013 *Nature* **493** 283
[2] Luo Z, Xu D and Wu S T 2014 *J. Disp. Technol.* **10** 526
[3] Luo Z, Chen Y and Wu S T 2013 *Opt. Express* **21** 26269
[4] Gu G and Forrest S R 1998 *IEEE J. Sel. Top. Quantum Electron.* **4** 83
[5] Kanno H, Hamada Y and Takahashi H 2004 *IEEE J. Sel. Top. Quantum Electron.* **10** 30
[6] Bardsley J N 2004 *IEEE J. Sel. Top. Quantum Electron.* **10** 3
[7] Cok R S 2004 *US Patent* 7259505
[8] Poitras D, Kuo C-C and Py C 2008 *Opt. Express* **16** 8003
[9] Goto S, Miyatake M and Saiki Y 2016 *SID Symp. Digest of Technical Papers* vol 47 p 513
[10] Singh R, Unni K N N, Solanki A and Deepak 2012 *Opt. Mater.* **34** 716
[11] Renault O, Salata O V, Etchells M, Dobson P J and Christou V 2000 *Thin Solid Films* **379** 195
[12] Lau K C, Xie W F, Sun H Y, Lee C S and Lee S T 2006 *Appl. Phys. Lett.* **88** 083507
[13] Xie W F, Sun H Y, Law C W, Lee C S, Lee S T and Liu S Y 2006 *Appl. Phys. A* **85** 95
[14] Lee J H, Liao C C, Hu P J and Chang Y 2004 *Synth. Met.* **144** 279
[15] Chiu T L, Lee J H, Hsiao Y P, Lin C F, Chao C C, Leung M K, Wan D H, Chen H L and Ho H C 2011 *J. Phys. D: Appl. Phys.* **44** 095102
[16] Xie W F, Zhao Y, Li C N and Liu S Y 2006 *Opt. Express* **14** 7954
[17] Li J-F, Su S-H, Hwang K-S and Yokoyama M 2007 *J. Phys. D: Appl. Phys.* **40** 2435
[18] Kim S-Y, Lee J-H, Lee J-H and Kim J-J 2012 *Org. Electron.* **13** 826
[19] Cho H and Yoo S 2012 *Opt. Express* **20** 1816
[20] Yang C J, Lin C L, Wu C C, Yeh Y H, Cheng C C, Kuo Y H and Chen T H 2005 *Appl. Phys. Lett.* **87** 143507
[21] Lee B D, Cho Y-H, Oh M H, Lee S Y, Lee S Y, Lee J H and Zang D S 2008 *Mater. Chem. Phys.* **112** 734
[22] Yang X, Mutlugun E, Dang C, Dev K, Gao Y, Tan S T, Sun X W and Demir H V 2014 *ACS Nano* **8** 8224
[23] Kim J-B, Lee J-H, Moon C-K, Kim S-Y and Kim J-J 2013 *Adv. Mater.* **25** 3571
[24] Mashford B S *et al* 2013 *Nat. Photon.* **7** 407
[25] Zhu R, Luo Z and Wu S T 2014 *Opt. Express* **22** A1783
[26] Neyts K J 1998 *Opt. Soc. Am. A* **15** 962
[27] Brütting W, Frischeisen J, Schmidt T D, Scholz B J and Mayr C 2013 *Phys. Status Solidi A* **210** 44
[28] Hofmann S, Thomschke M, Lüssem B and Leo K 2011 *Opt. Express* **19** A1250
[29] Liang H, Luo Z, Zhu R, Dong Y, Lee J-H, Zhou J and Wu S T 2016 *J. Phys. D: Appl. Phys.* **49** 145103
[30] Nakamura T, Tsutsumi N, Juni N and Fujii H 2005 *J. Appl. Phys.* **97** 054505
[31] Meyer J, Winkler T, Hamwi S, Schmale S, Johannes H H, Weimann T, Hinze P, Kowalsky W and Riedl T 2008 *Adv. Mater.* **20** 3839
[32] Coello C A C and Lamont G B 2004 *Applications of Multi-Objective Evolutionary Algorithms* (Singapore: World Scientific)
[33] Greiner H 2007 *Japan. J. Appl. Phys.* **46** 4125
[34] Ge Z B, Wu T X, Zhu X Y and Wu S T 2005 *J. Opt. Soc. Am. A* **22** 966